https://doi.org/10.5194/egusphere-2026-3088
Preprint. Discussion started: 3 August 2026

Development and Experimental Validation of a Reference-type Coherent Doppler Wind Lidar for Meteorological Operations

Zhichao Bu[1,2,3], Yaru Dai[1,2,3], Yuanyuan Huang[4], Yubao Chen[*,1,2,3] ,Zhigang Li[*,5], Guohua Jin[6],Xuliang Chen[6],

[1]CMA Research Centre on Meteorological Observation Engineering Technology,Beijing 100000,China
[2]Meteorological Observation Centre, China Meteorological Administration,Beijing 100000,China
[3]State Key Laboratory of Environment Characteristics and Effects for Near-space,Beijing 100000,China
[4]Bayannur Linhe Meteorological Bureau,Bayannur 015000,China
[5]School of Physics and Optoelectronic Engineering, Ludong University,Yantai 264005,China
[6]Southwest Institute of Technical Physics,Chengdu 610041,China

Correspondence to: *Yubao Chen (chenyb@cma.gov.cn),Zhigang Li (lizg@ldu.edu.cn).*

Abstract. In response to the urgent need for calibration technology in the application of wind lidar in the meteorological operations, this paper describes the development of a Reference-type Coherent Doppler Wind Lidar(RCDWL) for calibration. Based on a dual-channel composite detection mechanism combining continuous and pulsed modes, the RCDWL achieves key technical specifications including a low blind zone of 10 m, a high resolution of 10 m, and a maximum detection altitude of 3,000 m.To verify the performance and stability of the RCDWL, comparison experiments and data analyses were conducted using a radiosonde and a meteorological gradient tower, respectively. Comparison results with the radiosonde showed a wind speed systematic error of -0.05 m/s and a standard deviation of 1.11 m/s, while the wind direction systematic error was 1.34° with a standard deviation of 12.05°; the correlation coefficients were all higher than 0.97.Comparison results with the gradient tower showed a systematic error of 0.01 m/s and a standard deviation of 0.28 m/s for wind speed, and a systematic error of -0.09° and a standard deviation of 2.90° for wind direction, with correlation coefficients all exceeding 0.98.Based on these results, we used RCDWL as a reference source for a joint comparison and analysis of 9 lidars in meteorological operations. The results showed that the correlation coefficients for horizontal wind speed were greater than 0.98, with standard deviations less than 0.8 m/s; for wind direction, the correlation coefficients were greater than 0.97, with standard deviations less than 8°. Additionally, when using RCDWL as a reference standard source for the comparison and calibration of lidars prior to shipment, RCDWL effectively improves the product accuracy of lidars prior to shipment. These results fully validate the detection capabilities and stability of the RCDWL, establishing a stable and reliable reference benchmark for lidar calibration within the meteorological operations. The RCDWL fills a technical gap in wind lidar calibration reference sources and can be used for the comparison and calibration of Lidar equipment , holding great practical significance for enhancing the application level of wind lidars in various fields.

https://doi.org/10.5194/egusphere-2026-3088
Preprint. Discussion started: 3 August 2026

1 Introduction

Wind lidar has developed rapidly over the past few decades, offering advantages such as high spatio-temporal resolution, fast response times, and high observational accuracy. As the core equipment for acquiring high-resolution wind fields, Doppler wind lidar has been widely applied in atmospheric science research, meteorological early warning, aviation safety, renewable energy assessment, and military operations support (Jin et al., 2020; Zhai et al., 2017; YIM, 2020, Yuan et al., 2022) . Numerous domestic institutions have undertaken the development of wind lidars. With the increasing demands of China's meteorological monitoring operations, wind lidars have gradually been deployed and applied by meteorological and environmental protection agencies (Wang et al., 2020; Yang et al., 2023; Yuan et al., 2020). High-quality wind field data can improve the accuracy of model forecasts [Mariani et al., 2020], and conducting comparative calibration and measurement accuracy assessments for wind lidars is one of the key challenges that must be addressed for the operational application of lidars. Calibration methods for wind lidar include the standard wind tunnel method [Floris et al., 2017], flywheel calibration [Pedersen et al., 2021],and comparative observation methods [Lindong et al., 2020;Shu et al., 2016;Park et al., 2018;Luo et al., 2024;Päschke et al., 2014;Liu et al., 2020]. The standard wind tunnel method offers the advantages of traceability, high repeatability, and close approximation to real atmospheric conditions, but it is constrained by cost, flow field conditions, and equipment size. Flywheel calibration is characterized by low cost and high accuracy, but it cannot simulate real atmospheric echoes and struggles to reproduce three-dimensional wind fields. Comparative observation methods typically include meteorological gradient tower comparison, cross-comparison, and sounding comparison. The meteorological gradient tower comparison method verifies the accuracy of near-surface wind speed measurements through synchronized observations with equipment such as ultrasonic anemometers installed on meteorological towers [Lindong et al., 2020; Shu et al., 2016], and offers high reliability for near-surface wind speed measurements, but its detection range is limited by the height of the tower. The cross-calibration method involves synchronized observations using multiple lidars or other types of wind measurement equipment (such as wind profiler radars) to cross-validate the consistency of the equipment's observational results[Pearson et al., 2009,Päschke et al., 2014;Liu et al., 2020].The radiosonde comparison method verifies wind measurement accuracy across the entire detection range by comparing wind speed profiles obtained from radiosondes at different altitude layers. Among the representative devices for operational applications, L-band sounding radar can cover the entire atmosphere. Currently, the "radiosonde data comparison method" is commonly used both domestically and internationally to calibrate and analyze wind lidars[Park et al., 2018;Luo et al., 2024;Liu et al., 2020]; however, the inherent characteristics of the radiosonde mean that while it offers a long detection range, it has low observation frequency and limited measurement accuracy, making it difficult to meet the needs of high-resolution wind field observations. Furthermore, it is susceptible to balloon drift, resulting in limitations for high-resolution lidar comparison and validation.

In this paper, the Meteorological Observation Center of the China Meteorological Administration has developed a high-performance Reference-type Coherent Doppler Wind Lidar (RCDWL) for the comparison and calibration of wind lidars in the meteorological operations. Following its successful development, the RCDWL underwent comparisons and analyses

https://doi.org/10.5194/egusphere-2026-3088
Preprint. Discussion started: 3 August 2026

with radiosonde and gradient tower, with wind measurement accuracy reaching operational standards. Through practical calibration applications on operational lidars and lidars awaiting shipment, the RCDWL has demonstrated its high detection accuracy, stability, and reliability. It can serve as a reference for the operational calibration of meteorological wind lidars.

2 Development of the Lidar System

2.1 System Configuration and Technical Specifications

The RCDWL employs a continuous/pulsed coherent composite detection scheme, utilizing a 1.55 μm narrow-linewidth pulsed fiber laser—which is safe for the human eye—as its emission source. It addresses key technical challenges including continuous/pulse composite parallel detection, low-blind-zone detection, and high-resolution pulse detection. Figure 1 shows the main unit design (block diagram) and exterior view of the lidar, with its primary performance parameters listed in Table 1.Based on continuous/pulse composite parallel detection technology, the system can simultaneously acquire wind field data at both low and high altitudes, significantly enhancing data rate and spatiotemporal coverage capabilities. Combined with high-precision wind field inversion technology, it effectively resolves the trade-off between blind zones and range, as well as resolution and accuracy under narrow pulse width conditions, achieving meter-level low-blind-zone, high-resolution detection. Furthermore, through high-speed real-time data acquisition and processing coupled with VCM rapid focusing technology, the system reliably extracts Doppler shifts from the weak signal, ultimately endowing the coherent Doppler wind lidar with comprehensive high-performance capabilities characterized by high precision, high real-time performance, low blind zones, and maintenance-free operation.

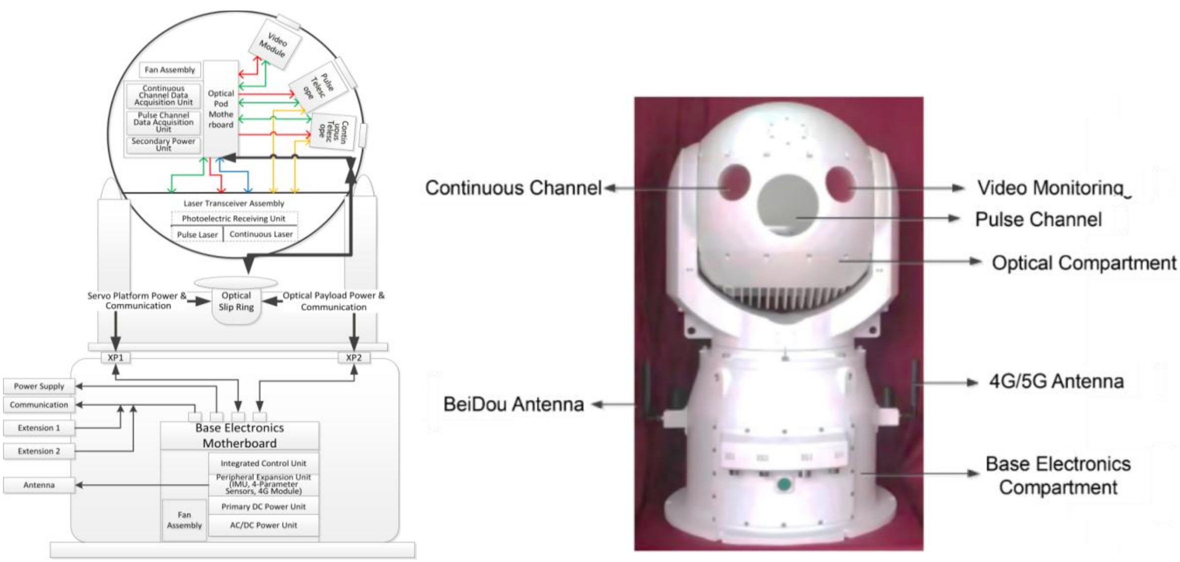

Figure 1: (a)Main unit design and block diagram of the RCDWL;(b)Physical photo and main components of the RCDWL

Table 1: Key performance specifications of the RCDWL

Wind Profile Mode		
1.1	Operating mode	Coherent detection system
1.2	Minimum detection height	≤10 m
1.3	Maximum detection height	≥3000 m (under clear weather conditions)
1.4	Height resolution	10 m, 30 m, 50 m, etc. (configurable)
1.5	Wind direction range	0–360°
1.6	Wind speed range	0 m/s to 75 m/s
1.7	Wind speed error	≤0.4 m/s
1.8	Wind direction error	≤3°
1.9	Vertical airflow error	≤0.1 m/s
1.10	Data refresh rate	3s–10min (configurable)
Scan detection mode		
2.1	Minimum radial detection distance	10 m
2.2	Maximum radial detection distance	6 km (elevation angle ≤ 6°)
2.3	Range resolution	10 m, 30 m, 50 m, 75 m, 100 m (user-configurable)
2.4	Radial data refresh time	≤2 s
2.5	Radial wind speed resolution	≤ 0.1 m/s
2.6	Scan angle resolution	0.05°

2.2 Continuous/Pulse Composite Parallel Detection Technology

To address the detection requirements for the 10-meter low-altitude blind zone and mid-to-high-altitude wind fields, a continuous/pulse composite multimode laser integrated transmission technology is employed [Zhang et al., 2019]. In the low-altitude range (10 m–100 m), the laser output from the fiber is collimated and focused within the near-field range (10 m–60 m) via a zoom telescope using continuous coherent detection mode, achieving a minimum distance resolution of 10 m;In the mid-to-high altitude range (100 m–3,000 m), wind field detection is performed in pulse coherent detection mode, achieving a minimum distance resolution of 30 m. This dual-detection mechanism for low and high altitudes enhances both the data acquisition rate and distance resolution.The entire system employs integrated continuous-pulse dual-mode laser transmission technology to achieve stable and reliable adaptive amplification of continuous-pulse lasers and compact, integrated dual-mode laser transmission, as shown in Figure 2. The optical path utilizes flexible optical fibers to construct a highly sensitive coherent optical system, creating a compact and streamlined optical architecture. This efficiently enables integrated transmission and reception of multimode lasers along with adaptive optical path detection, meeting the high signal-to-noise ratio detection requirements for the distinct characteristics of multimode atmospheric echoes.

https://doi.org/10.5194/egusphere-2026-3088
Preprint. Discussion started: 3 August 2026

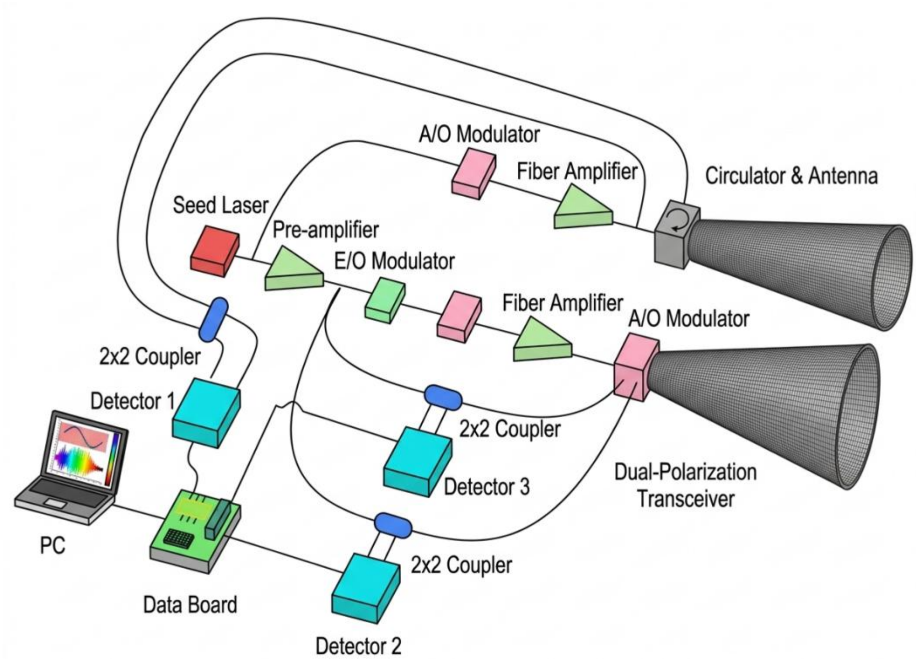

Figure 2: High-efficiency parallel transmission and reception optical path for continuous/pulsed composite operation

For the transmission section, a continuous-wave/pulsed co-narrow-linewidth light source and a parallel amplification multimode operating mode are employed. Through efficient fiber beam splitting, multimode synchronous modulation via an acousto-optic modulator (AOM), and low-noise multi-stage fiber amplification, the system achieves low-noise, continuous/pulsed dual-channel multimode synchronous modulation transmission. A dual-antenna configuration is employed to effectively avoid the range measurement issues caused by mismatches in the theoretical design of near-field and far-field optical antenna aberrations inherent in traditional single-antenna approaches. In the receiver section, the echo signals from the continuous-wave and pulsed channels are detected separately. An optical circulator and a fiber-optic circulator are used to separate the transmitted laser and the echo light, and beat mixing between the echo light and the local oscillator light is performed in fiber-optic couplers, followed by photodetection and conversion using balanced detectors.

2.3 High-Precision Wind Field Inversion Technology

This system employs an 8-beam scanning strategy based on the VAD method, utilizing multi-beam spatial adaptive scanning and short-time adaptive weighting inversion algorithms to improve wind field inversion accuracy. The workflow is shown in Figure 3.

https://doi.org/10.5194/egusphere-2026-3088
Preprint. Discussion started: 3 August 2026

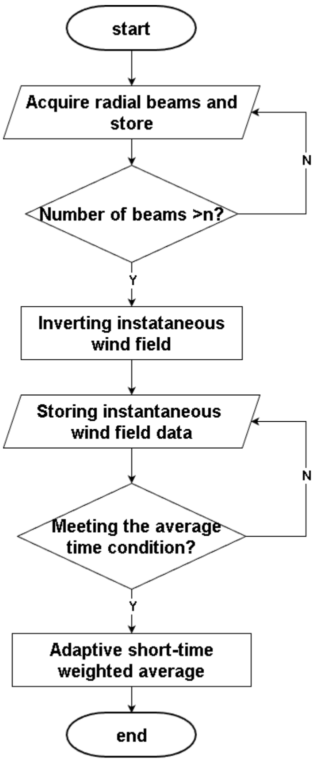

Figure 3: Process flow for multi-beam spatial adaptive scanning and short-term adaptive weighting inversion

The three-dimensional vector of the wind field is calculated by solving a system of overdetermined multi-beam equations, as shown in Equation (1), and the meteorological horizontal wind speed, horizontal wind direction, and vertical airflow are computed.

$$\begin{gathered} v_{xj} \cdot \sin\alpha_{g1j} \cdot \cos\beta_{g1j} + v_{yj} \cdot \cos\alpha_{g1j} \cdot \cos\beta_{g1j} + v_{zj} \cdot \beta_{g1j} = v_{r1j} \\ v_{xj} \cdot \sin\alpha_{gij} \cdot \cos\beta_{gij} + v_{yj} \cdot \cos\alpha_{gij} \cdot \cos\beta_{gij} + v_{zj} \cdot \beta_{gij} = v_{rij} \\ \vdots \\ v_{xj} \cdot \sin\alpha_{gnj} \cdot \cos\beta_{gnj} + v_{yj} \cdot \cos\alpha_{gnj} \cdot \cos\beta_{gnj} + v_{zj} \cdot \beta_{gnj} = v_{rnj} \end{gathered} \quad (1)$$

where j represents the inversion cycle, i = 1, …, n, represents the i-th radial velocity in the j-th inversion cycle,v_{xj},v_{yj}andv_{zj} represent the three-dimensional wind field vector in the j-th inversion cycle, $\alpha_{gij}$and β_{gij} represent the i-th beam azimuth and beam elevation angle in the j-th inversion cycle, respectively.

When averaging wind profile data, the instantaneous wind profile data within the averaging time window is divided into multiple time segments using adaptive partitioning, and differentiated weights are assigned to the instantaneous wind profile data of different segments, as shown in Equation (2), with weights increasing as the segment approaches the current time, and the weight factor a_i summing to 1.

$$V_{xavg} = \sum_{i=0}^{n} V_{xi} \cdot a_i$$

$$V_{yavg} = \sum_{i=0}^{n} V_{yi} \cdot a_i \quad (2)$$

https://doi.org/10.5194/egusphere-2026-3088
Preprint. Discussion started: 3 August 2026

$$V_{zavg} = \sum_{i=0}^{n} V_{zi} \cdot a_i$$

We conducted error simulation calculations based on multi-beam spatial adaptive scanning and short-time adaptive weighting inversion algorithms. The radial wind speed error is set at ±0.048 m/s (system signal acquisition and processing accuracy), with a scanning beam pitch angle of 70°. Additionally, a 0.3° error is applied to both the laser beam scanning azimuth and pitch angles. The inversion process utilizes eight beams and 10-minutes of average data, with results presented in Figure 4-5. The simulation yields errors of ≤0.154 m/s (V ≤ 10 m/s) and ≤1.54%V (V> 10 m/s) for wind speed, and ≤1.24° for wind direction.

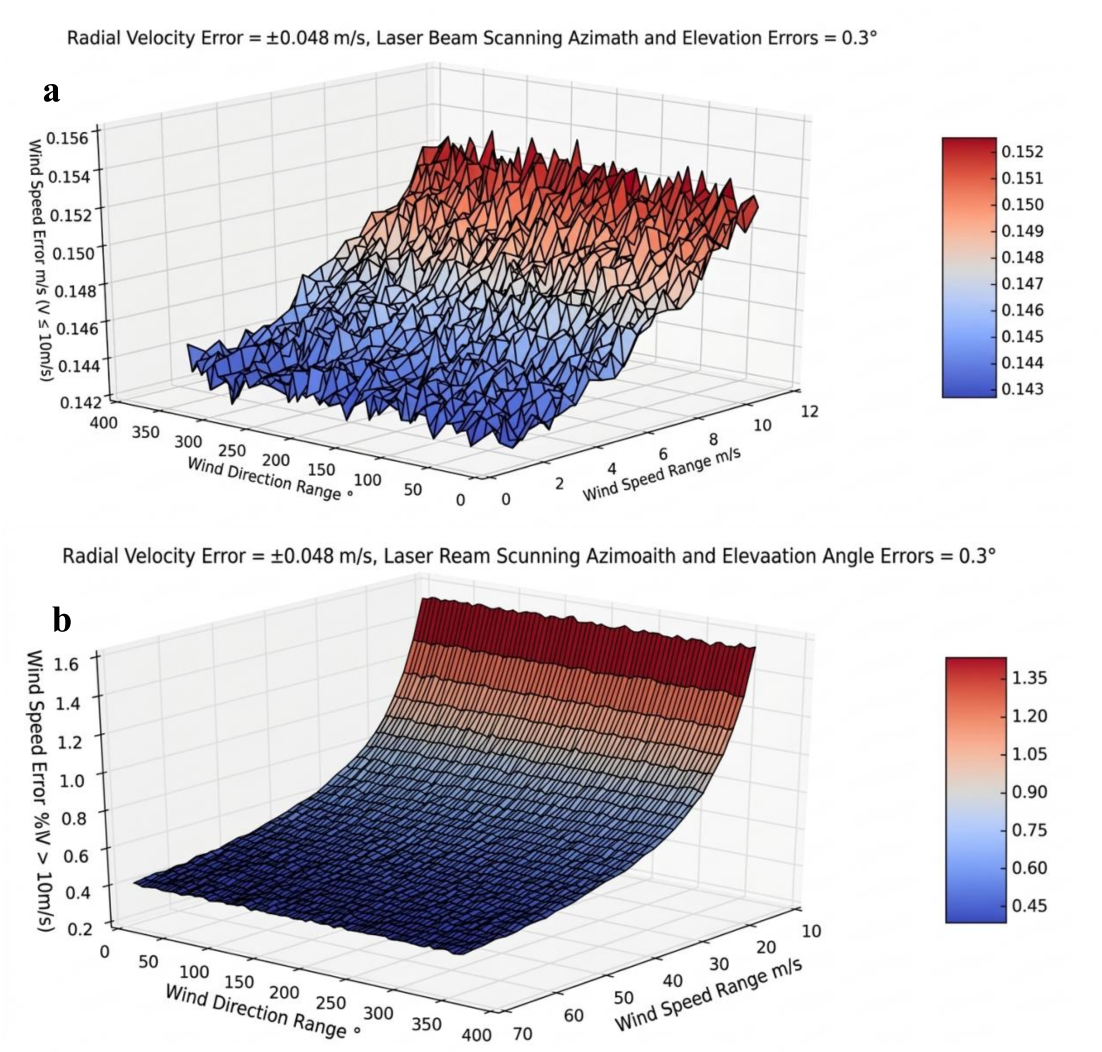

Figure 4 Simulation of wind speed error for the wind lidar under wind speed range V ≤ 10 m/s(a) and V > 10 m/s(b).

https://doi.org/10.5194/egusphere-2026-3088
Preprint. Discussion started: 3 August 2026

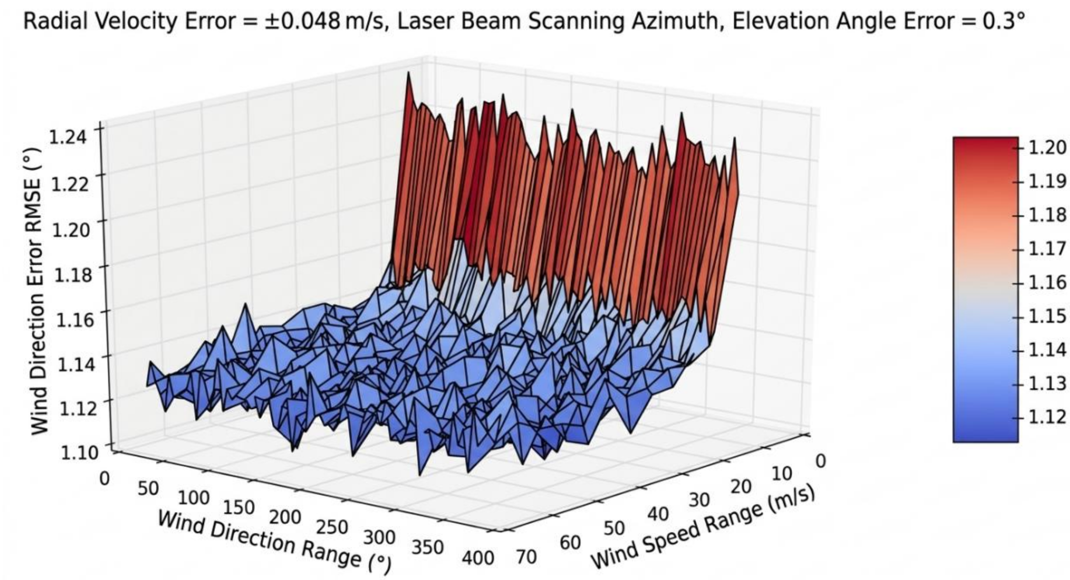

Figure 5 Simulation of wind direction error for the wind lidar

3 Wind Measurement Comparison and Data Analysis

3.1 Data Analysis Methods

This study employs a unified method to perform error calculation and analysis for the RCDWL in comparison with radiosonde, gradient tower, and operational lidars, in order to verify its accuracy in comparison.

At the same or similar measurement altitude layers, valid data samples from the comparison devices were simultaneously selected to calculate the comparison errors according to Equations (3), (4) and (5), including systematic errors (X), standard deviations (S), and correlation coefficients (R).

The detailed calculation formulas are as follows:

$$X = \frac{\sum_{i-1}^{n}(a_i - b_i)}{n} \qquad (3)$$

$$S = \sqrt{\frac{\sum_{i=1}^{n}(x_i - \bar{x})^2}{n-1}} \qquad (4)$$

$$R = \frac{\sum_{i=1}^{n}(a_i - \bar{a}_i)(b_i - \bar{b}_i)}{\sqrt{\sum_{i=1}^{n}(a_i - \bar{a}_i)^2}\sqrt{\sum_{i=1}^{n}(b_i - \bar{b}_i)^2}} \qquad (5)$$

In the equation, a_i represents the wind measurements from Device 1; b_i represents the wind measurements from Device 2; n represents the number of measurements; X represents the systematic error; S represents the standard deviation ; and R represents the correlation coefficient.

https://doi.org/10.5194/egusphere-2026-3088
Preprint. Discussion started: 3 August 2026

3.2 Comparison with Radiosonde

From December 2023 to March 2024, the RCDWL was deployed for a four-month field trial at the Beijing Daxing Experimental Base of the Meteorological Observation Center. Synchronous collocated observations were performed with the radiosonde measurements to evaluate the observational accuracy of the RCDWL. The supporting L-band sounding radar was employed to acquire routine wind profile data during the experiment. The RCDWL output a set of data products every 10 minutes. The differences between the RCDWL and the radiosonde were analyzed, including the correlation coefficients, systematic errors, and standard deviations for wind speed and wind direction.

During the field campaign, a total of 87 valid synchronous comparison groups were obtained through routine balloon release operations. RCDWL data that were affected by weather conditions such as dense fog and precipitation were excluded, and statistical analysis was performed on all data within the RCDWL's measurement altitude range. The results are shown in Figure 6. The comparison results between the RCDWL and the radiosonde demonstrated good consistency, with a systematic error of -0.05 m/s and a standard deviation of 1.11 m/s for wind speed; the systematic error for wind direction was -1.34°, with a standard deviation of 12.05°, and the correlation coefficients were all above 0.97. Overall, the comparison tests with the radiosonde demonstrated good agreement in data results across the entire detection range, fully validating the reliability and accuracy of the RCDWL in meteorological detection, and providing robust data support for meteorological monitoring and forecasting.

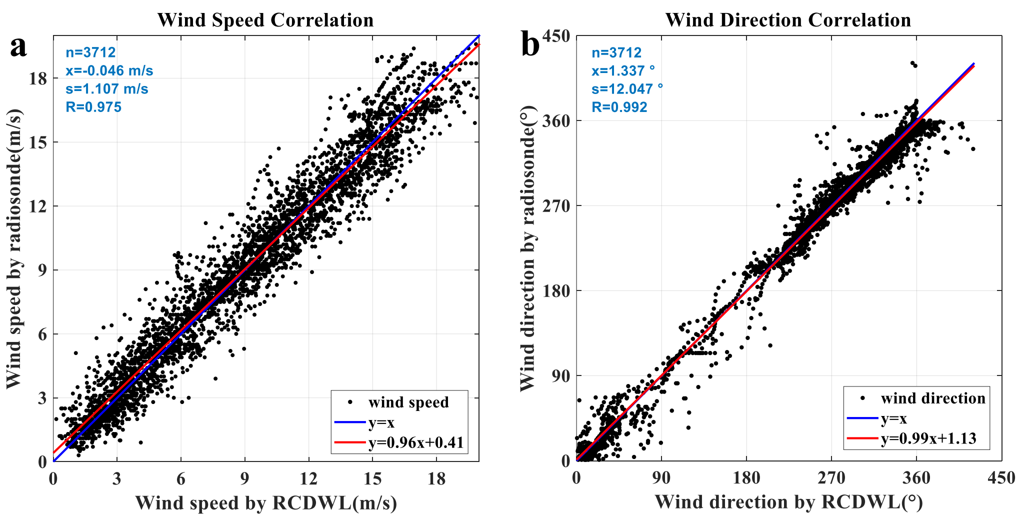

Figure 6 Consistency analysis of wind speed(a)and wind direction(b) between RCDWL and radiosonde observational data

3.3 Comparison with the Gradient Tower

From April 19, 2024, to May 4, 2024, we conducted validation tests comparing the RCDWL with the gradient tower at the Shiyan Meteorological Observation Station in Shenzhen.

https://doi.org/10.5194/egusphere-2026-3088
Preprint. Discussion started: 3 August 2026

The Shenzhen meteorological gradient observation tower has a mast height of 356 meters and features 35 observation platforms spaced 10 meters apart. The comparison equipment used was a mechanical anemometer, specifically the WMT700 model manufactured by VASALA. Its wind speed measurement range is 0.4–75 m/s, with a start-up threshold of <0.5 m/s and a wind speed accuracy of 0.2 m/s. The wind direction measurement range is 0–360°, with a resolution of 1° and an accuracy better than ±2°.During synchronized observations, the RCDWL was positioned at the same height as the base of the meteorological gradient tower, with a horizontal distance of less than 50 m, as shown in Figure 7. Using the meteorological gradient tower's time as the reference, 10-minute average wind speed and direction data were obtained at 7 levels (10 m, 20 m, 50 m,100 m, 150 m, 200 m, and 300 m).

Figure 7: Comparison of the Gradient Tower and RCDWL at the Shenzhen observation site

Figure 8 shows the time-series comparison between measurements from the RCDWL(Prod.No.:YKL-B01) and the meteorological gradient tower at heights of 10 m and 200 m throughout the comparison period. Figures 9 and 10 present scatter plots of the 10-minute average wind speed and wind direction data at the two height levels, demonstrating good consistency between the two datasets.

https://doi.org/10.5194/egusphere-2026-3088
Preprint. Discussion started: 3 August 2026

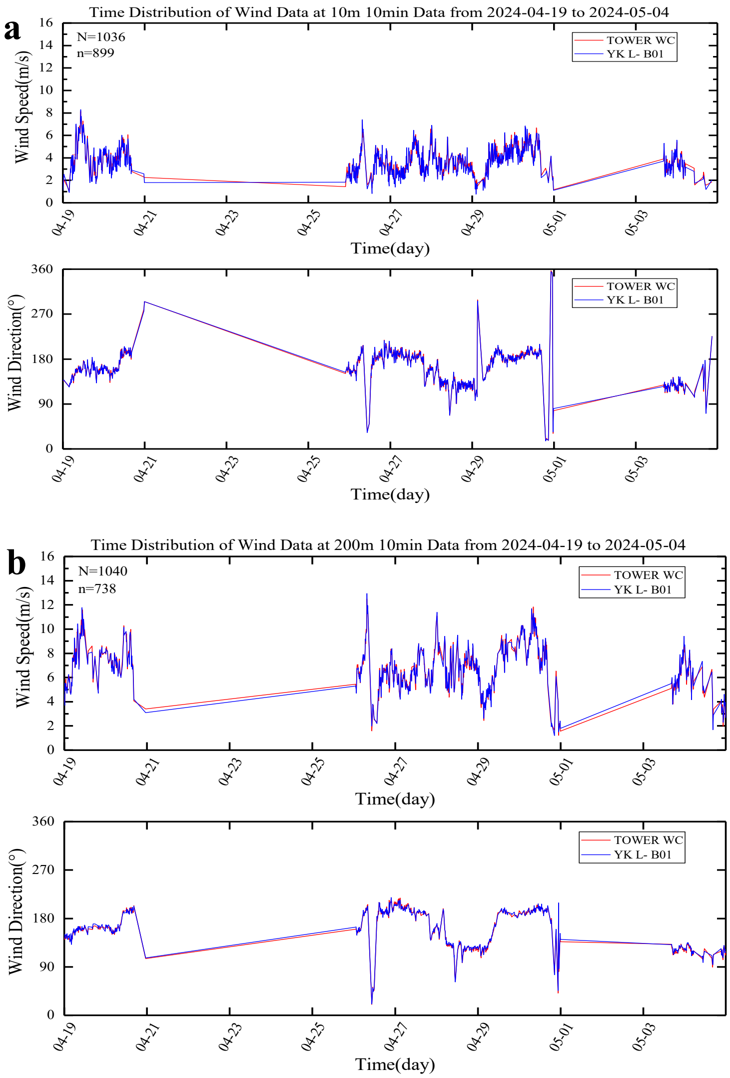

Figure 8: Time-series plots of 10-minute average wind speed and direction data at heights of 10 m(a) and 200 m(b)

https://doi.org/10.5194/egusphere-2026-3088
Preprint. Discussion started: 3 August 2026

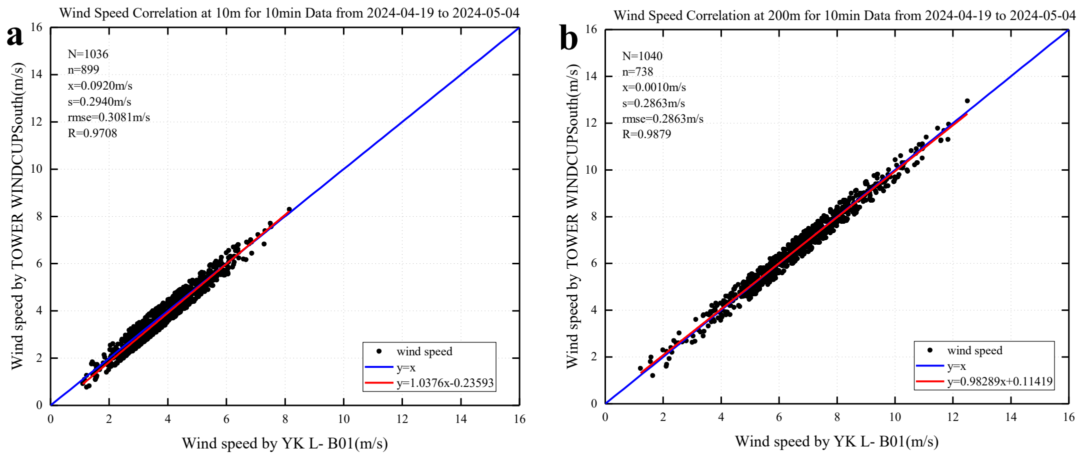

Figure 9: Scatter plots of 10-minute average wind speeds at heights of 10 m(a) and 200 m(b)

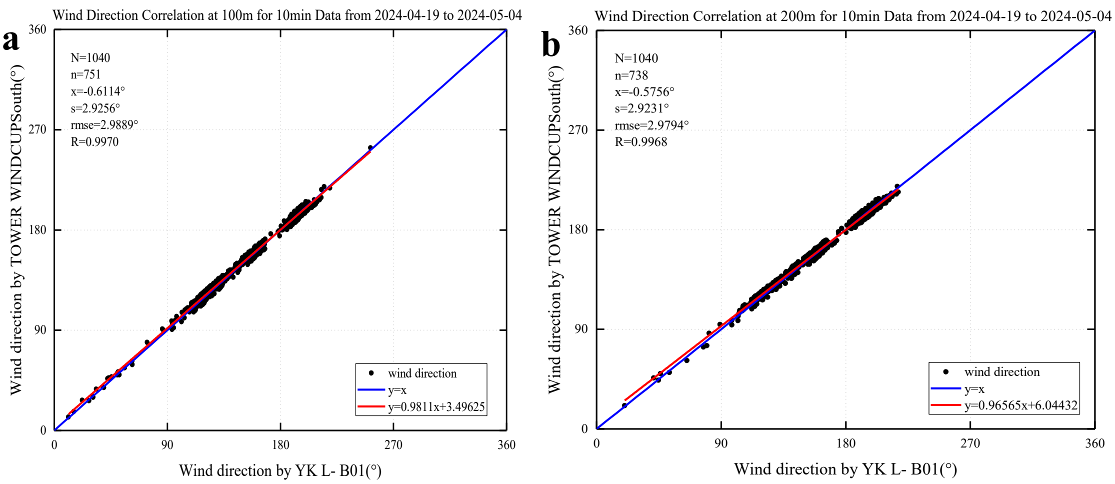

Figure 10: Scatter plots of 10-minute average wind direction at heights of 10 m(a) and 200 m(b)

Statistical analysis of the comparison results at each height is summarized in Table 2. The systematic error in wind speed between the gradient tower and the RCDWL is 0.01 m/s, with a standard deviation of 0.28 m/s and a correlation coefficient of 0.98. The systematic error in wind direction is -0.09°, with a standard deviation of 2.90° and a correlation coefficient of 0.99. The comparison accuracy metrics are close to those of mechanical anemometers.

Table 2: Statistical comparison results of wind speed and direction between the gradient tower and RCDWL

	Wind Speed			Wind Direction		
Altitude (m)	Systematic Error (m/s)	Standard Deviation (m/s)	Correlation Coefficient	Systematic Error (°)	Standard Deviation (°)	Correlation Coefficient

https://doi.org/10.5194/egusphere-2026-3088
Preprint. Discussion started: 3 August 2026

10	0.0920	0.2940	0.9708	0.0550	2.9495	0.9958
20	-0.0007	0.2729	0.9742	-0.5197	2.9693	0.9961
50	0.0656	0.2819	0.9854	0.6171	2.9280	0.9968
100	0.0228	0.2955	0.9887	-0.6114	2.9256	0.9970
150	-0.1384	0.2552	0.9894	0.1737	2.7001	0.9971
200	0.0010	0.2863	0.9879	-0.5756	2.9231	0.9968
300	0.0433	0.2891	0.9896	0.2659	2.9136	0.9963
Average	0.0122	0.2822	0.9837	-0.0850	2.9013	0.9965

To quantitatively evaluate the wind measurement performance of the RCDWL, we conducted a comparative analysis of its accuracy metrics (standard deviation) against those of 66 operational lidars tested at the Shenzhen Meteorological Gradient Tower. The results are illustrated in a box-and-whisker plot (Fig.11).In this figure, the box represents the quartile distribution of the accuracy data for the 66 lidar units; the horizontal line inside the box is the median, and the upper and lower boundaries correspond to the upper and lower quartiles, respectively; the red dots represent the measured accuracy of the RCDWL. It can be seen that the RCDWL's standard deviation for wind speed measurements ranks in the top 9.1% among all devices, while its standard deviation for wind direction measurements ranks in the top 1.5%, indicating that the RCDWL possesses significant advantages in both wind speed and wind direction measurement accuracy.

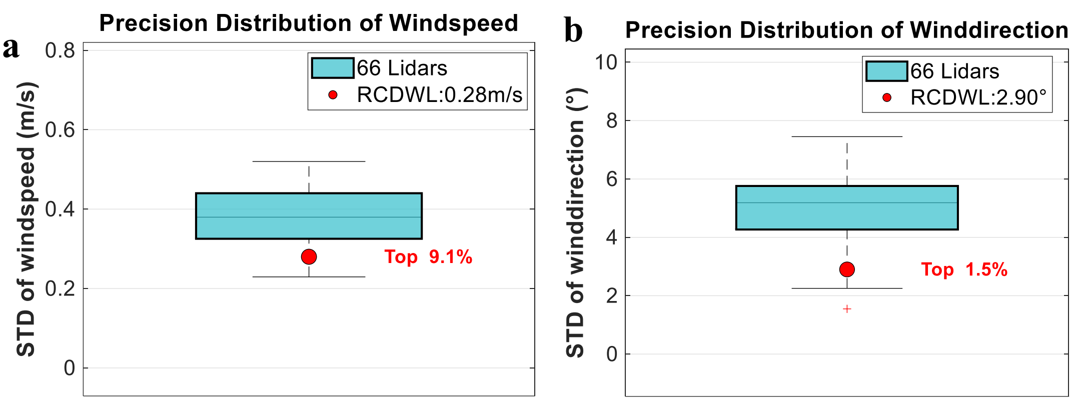

Figure 11: Precision distribution of wind speed(a) and wind direction(b) between the RCDWL and 66 Operational lidars

4 Applications of the RCDWL

4.1 Joint Comparison Analysis

From December 16, 2023, to January 14, 2024, the RCDWL served as a quantitative reference lidar and participated in a joint comparison of operational lidars used for routine observations. This comparison involved nine in-situ operational lidars, all of which had previously completed comparison and validation with a radiosonde; the entire comparison duration lasted one month.Using RCDWL's wind profile data as the reference source, at a 10-minute temporal resolution and the same

https://doi.org/10.5194/egusphere-2026-3088
Preprint. Discussion started: 3 August 2026

spatiotemporal resolution, an example of the wind profile comparison results is shown in Figure 12. Additionally, the measurement results from a radiosonde were included as a qualitative reference. The wind profile results from the nine lidars under test showed good consistency with those of the RCDWL. Consistency analyses were conducted separately for the data from each of the nine lidars under test and the RCDWL data. The results are shown in Table 3. For all nine lidars, the correlation coefficients for horizontal wind speed were all greater than 0.98, with standard deviations all less than 0.8 m/s; the correlation coefficients for wind direction were all greater than 0.97, with standard deviations generally less than 8°.These performance metrics serve as the operational licensing criteria for coherent Doppler wind lidars in the meteorological operations under the China Meteorological Administration, indicating that the RCDWL can serve as a reference source and provide robust support for the calibration of wind lidars in the meteorological sector.

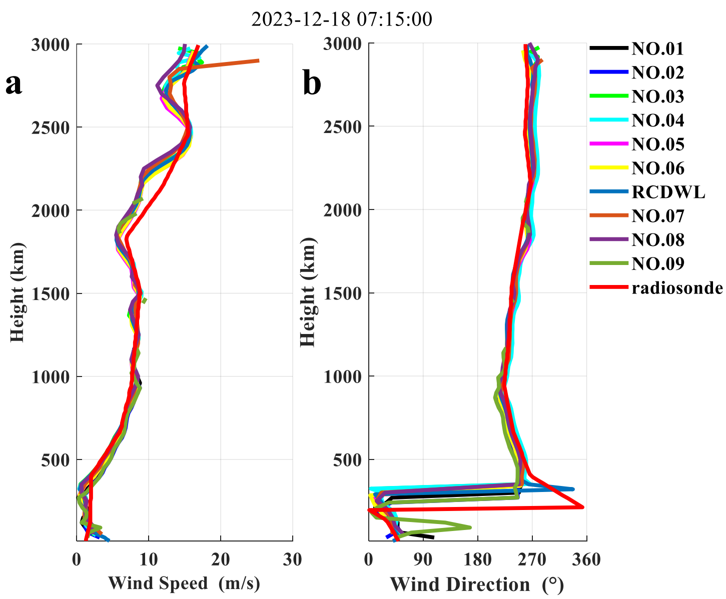

Figure 12:Comparison of wind speed profile(a) and wind direction profile(b) between the RCDWL and the on-site lidar

Table 2 Statistical results of the joint comparison of observations

Result\Radar ID		NO.1	NO.2	NO.3	NO.4	No. 5	No. 6	No. 7	No. 8	No. 9
Horizontal wind speed	System error	0.028	0.128	0.23	0.226	0.283	0.404	0.177	0.101	0.415
	Standard deviation	0.177	0.315	0.439	0.426	0.595	0.76	0.369	0.358	0.72
	Correlation coefficient	0.999	0.998	0.995	0.995	0.99	0.984	0.995	0.997	0.986
Horizontal wind direction	System error	5.965	8.135	0.156	-1.972	3.849	2.819	2.499	0.168	-3.063
	Standard deviation	2.444	4.882	5.541	5.147	7.595	9.406	4.268	3.913	8.853
	Correlation coefficient	0.999	0.995	0.992	0.992	0.983	0.973	0.995	0.996	0.976

https://doi.org/10.5194/egusphere-2026-3088
Preprint. Discussion started: 3 August 2026

4.2 Factory Calibration of lidars

To ensure the accuracy of wind measurement data from the domestic wind lidar network, the RCDWL, serving as a reference standard source, was used multiple times in 2025 for comparison and calibration of lidars prior to shipment. Figure 13 shows the scatter plot of measurement errors for a manufacturer's pre-shipment lidar before and after comparison and calibration with RCDWL in June 2025, with a time resolution of 10 minutes. Based on the comparison results with the RCDWL, by correcting the zero-height calibration error and enhancing data quality control of the pre-shipment lidar, the standard deviation of horizontal wind speed for the tested lidar was improved from 0.96 m/s to 0.68 m/s, and the standard deviation of wind direction was improved from 19.93° to 7.64°, resulting in a significant enhancement in detection accuracy. Using the RCDWL as a calibration reference source can rapidly and effectively improve the detection accuracy of domestic lidars.

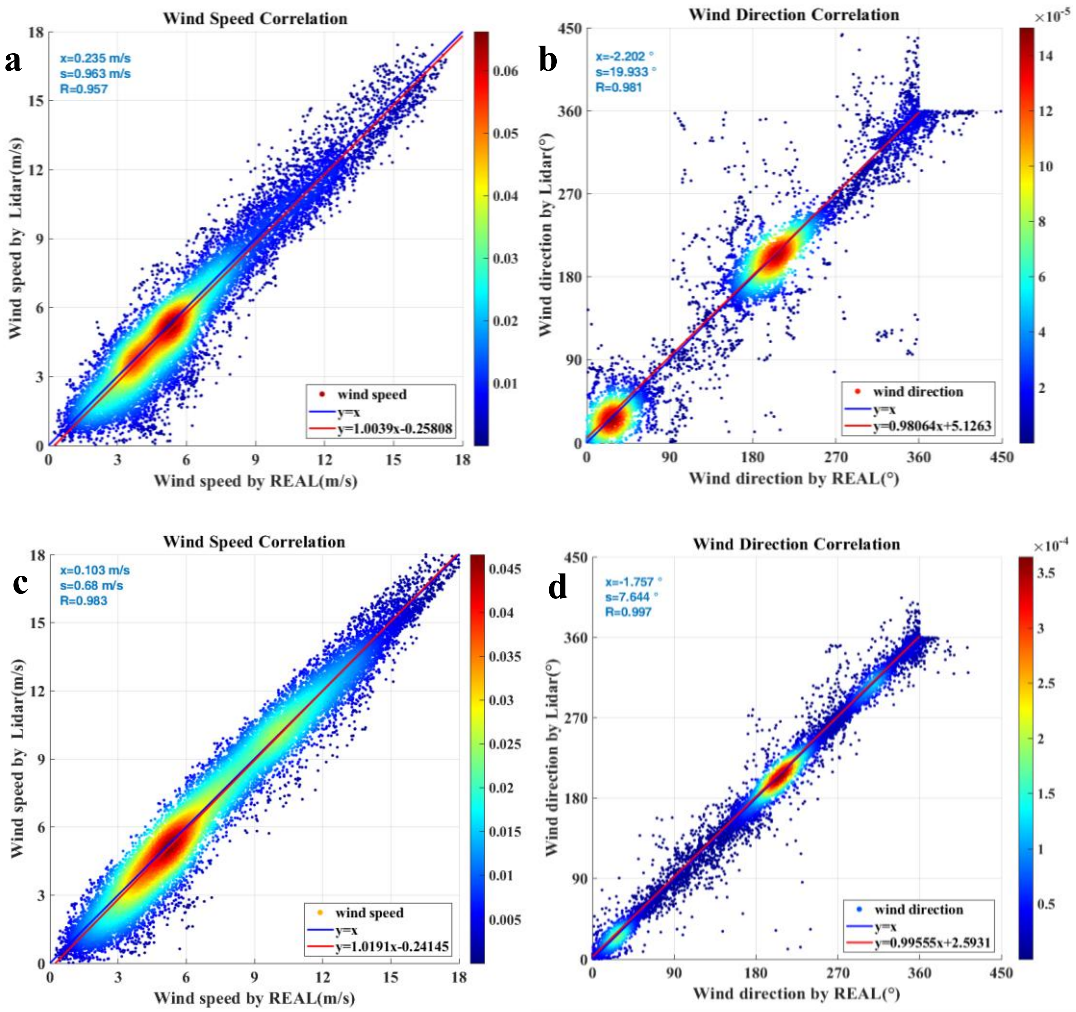

https://doi.org/10.5194/egusphere-2026-3088
Preprint. Discussion started: 3 August 2026

Figure 13:Comparison of measurement errors, including scatter plots of wind speed(a) and wind direction(b) before calibration and wind speed(c) and wind direction(d) after calibration

5 Summary

This study successfully developed a high-performance reference lidar system the RCDWL suitable for calibrating wind lidars in the meteorological operations and conducted systematic experimental validation of the system. The RCDWL employs a dual-channel composite detection mechanism combining continuous and pulsed modes, achieving key technical specifications such as a 10-meter low-blind-zone, 10-meter resolution, and a detection height of 3,000 meters, while demonstrating excellent environmental adaptability and stability. Comparison experiments with the radiosonde and the gradient tower validated the high accuracy and reliability of this reference lidar. In comparisons with the radiosonde, the correlation coefficients for wind speed and wind direction were both greater than 0.98. In comparisons with the gradient tower, the systematic error for wind speed was 0.01 m/s with a standard deviation of 0.28 m/s, and for wind direction, the systematic error was -0.09° with a standard deviation of 2.90°; all correlation coefficients exceeded 0.98.When used as a reference standard source for the comparison and calibration of operational lidars and lidars awaiting shipment, the RCDWL can achieve calibration errors of less than 0.8 m/s for horizontal wind speed and less than 8° for wind direction. In summary, the RCDWL is a wind lidar with high-performance specifications that meets the calibration parameter requirements for wind lidars in domestic meteorological applications. It has been successfully applied in the comparison and calibration of industry wind lidars and can serve as a reference standard for industry licensing evaluations when verifying equipment, thereby enhancing the calibration standards for wind lidars in meteorological applications.

Data Availability Statement

The data presented in this study are available on request from the corresponding author. The data are not publicly available due to privacy reason.

Author contributions

Y. C. conceptualized the research, and provided overall supervision. Z. B.,Y. D. and Z. L. was responsible for the research design, performing the experiments, data collection and processing, and drafting the manuscript. G. J., X. C. contributed to the maintenance and management of the instruments. Y. C. and Z. L. performed the data analysis and results discussion, contributed to the critical revision of the manuscript and approved the final version.All authors have read and agreed to the published version of the manuscript.

Acknowledgements

This research was supported by National Natural Science Foundation of China Grant U2442214.

References

Jin, X. M., Zhu, W. Y., and Liu, Q.: Application research of laser coherent wind technology, Journal of Atmospheric and Environmental Optics,15 ,161-173, https://doi.org/10.3969/j.issn.1673-6141.2020.03.001, 2020.

Zhai, X. C., Wu, S. H., and Liu, B. Y.: Doppler lidar investigation of wind turbine wake characteristics and atmospheric turbulence under different surface roughness, Optics Express, 25,A515-A529,, https://doi.org/10.1364/OE.25.00A515, 2017.

YIM, S.H.L.:Development of a 3D Real-Time Atmospheric Monitoring System (3DREAMS) Using Doppler LiDARs and Applications for Long-Term Analysis and Hot-and-Polluted Episodes,Remote Sens. 12, 1036. https://doi.org/10.3390/rs12061036,2020.

Yuan, J., Su, L., Xia, H., Li, Y., Zhang, M., Zhen, G., Li, J.: Microburst, Windshear, Gust Front, and Vortex Detection in Mega Airport Using a Single Coherent Doppler Wind Lidar, Remote Sens. 14, 1626. https://doi.org/10.3390/rs14071626,2022.

Wang, KX., Gao, CQ., Lin, ZF., Wang, Q., Gao, MW., Huang,S., and Chen, CY.: 1645 nm coherent Doppler wind lidar with a single-frequency Er:YAG laser, Optics Express, 28,14694-14704, https://doi.org/10.1364/OE.392092, 2020.

Yang, YW., Song, XQ., Lian, WC., Kang, BS., and Miao, CH.: Characteristics of Sea-Land Breeze in Huludao during Spring, 2021 and Its Impacts on Ozone Pollution,Acta Optica Sinica,,43,1228002, http://dx.doi.org/10.3788/AOS221607, 2023.

Yuan, JL., Xiao, HY., Wei, TW., Wang, L., Yue, B., and Wu, YB.: Identifying cloud, precipitation, windshear, and turbulence by deep analysis of the power spectrum of coherent Doppler wind lidar, Optics Express, 28,37406-37421, https://doi.org/10.1364/OE.412809, 2020.

Mariani, Z., Crawford, R., Casati, B., and Lemay, F.: A Multi-Year Evaluation of Doppler Lidar Wind-Profile Observations in the Arctic, Remote Sensing, 12,323, https://doi.org/10.3390/rs12020323, 2020.

Floris, v, D. M., Campagnolo, F., Jöholm, M., Angelou, M., Mikkelsen, T., and Kühn, M.: Demonstration and uncertainty analysis of synchronised scanning lidar measurements of 2-D velocity fields in a boundary-layer wind tunnel, Wind Energy Science, 2,329-341, https://doi.org/10.5194/wes-2-329-2017, 2017.

Pedersen, A. T., Courtney, M.: Flywheel calibration of a continuous-wave coherent Doppler wind lidar, Atmospheric Measurement Techniques,14, 889-903, https://doi.org/10.5194/amt-14-889-2021, 2021.

https://doi.org/10.5194/egusphere-2026-3088
Preprint. Discussion started: 3 August 2026

Lindong, D., Jinyuan, X., Hongchao, Z., Yongxiang, M., Lei, Z., Xinrui, W., Yongjing, M., Danjie, J., and Fangkun, W.: Multilevel validation of Doppler Wind lidar by the 325 m meteorological tower in the planetary boundary layer of Beijing, Atmosphere, 2020, 11, 1051, https://doi.org/10.3390/atmos11101051, 2020.

Shu, Z. R,, Li, Q. S., He, Y. C., and Chan P. Y.: Observations of offshore wind characteristics by Doppler-LiDAR for wind energy applications, Applied Energy, 169,150-163, https://doi.org/10.1016/j.apenergy.2016.01.135, 2016.

Park, S., Kim, SW., Park, MS., and Song, CK.: Measurement of Planetary Boundary Layer Winds with Scanning Doppler Lidar, Remote Sensing, 10,1261, https://doi.org/10.3390/rs10081261, 2018.

Luo, ZX., Song, XQ., Yin, JP., Bu, ZC., Chen, YB., Yu, YT., and Zhang, ZL.: Comparison and Verification of Coherent Doppler Wind Lidar and Radiosonde Data in the Beijing Urban Area, Advances in Atmospheric Sciences, 41,1865-1878, https://doi.org/ 10.1007/s00376-024-3240-9, 2024.

Pearson G., Davies F., Collier C.: An analysis of the performance of the UFAM pulsed Doppler lidar for observing the boundary layer,Journal of Atmospheric and Oceanic Technology, 26, 240-250,https://doi.org/10.1175/2008JTECHA1128.1,2009.

Päschke E., Leinweber R., Lehmann V. : A one year comparison of 482 MHz radar wind profiler, RS92-SGP Radiosonde and 1.5 µm Doppler Lidar wind measurements. Atmospheric Measurement Techniques Discussions, 7,439−11 479, https://doi.org/10.5194/amtd-7-11439-2014,2014.

Liu, H., Yuan, LC., Fan, CH., Liu, FF., Zhang, X., Zhu, XP., Liu, JQ., Zhu, XL., and Chen, WB.: Performance validation on an all-fiber 1.54-µm pulsed coherent Doppler lidar for wind-profile measurement, Optical Engineering, 59,014109, https://doi.org/ 10.1117/1.OE.59.1.014109, 2020.

Zhang YC. , Rui XB. , Guo P. Chen SY.,Li T.,Li BW.,:High power all-fiber laser with switchable pulsed and continuous operation modes for wind lidar. Proc. SPIE 11063, Pacific Rim Laser Damage,2019:Optical Materials for High-Power Lasers,11063,166-171,https://doi.org/10.1117/12.2539886,2019.